Simulating light atomic nuclei in a quantum computer

Author: Arnau Morón Rodríguez
*Facultat de Física, Universitat de Barcelona, Diagonal 645, 08028 Barcelona, Spain.**
Advisor: Javier Menéndez †

Abstract: Solving the dynamics of many-body systems is one of the most challenging problems in modern science. For this application, classical computational techniques face significant limitations, mainly the need to handle large Hilbert spaces. Quantum computation, particularly through hybrid quantum and classical algorithms, has started gaining popularity, offering a promising new approach. This work characterizes the Adaptive Derivative-Assembled Pseudo-Trotter ansatz Variational Quantum Eigensolver (ADAPT-VQE) algorithm by simulating ^{6}Be, ^{12}C and ^{14}N nuclei via the shell model on an ideal quantum computer. It focuses on the ADAPT-VQE's response to the inherent statistical noise that results from the finite number of measurements ("shots") performed. In particular, the study quantifies the energy convergence with measurement shots, while demonstrating how statistical noise impacts variational parameter optimization. The results show that this impact leads to a final energy error that scales with N_{shots} following a power law distinct from the standard statistical limit and particular for each nucleus. Furthermore, the mean energy converges towards the ideal value as the optimizer performs more effectively as N_{shots} increases.
Keywords: Quantum computing, nuclear shell model, VQE
SDGs: Quality education, Affordable and clean energy and Industry, innovation, infrastructure

I. INTRODUCTION

Understanding the collective behaviour of many interacting particles is a fundamental goal of modern science, with profound implications from nuclear physics to quantum chemistry [1]. The main difficulty in many-body physics is correctly describing the complex interactions between particles, a challenge that is due to the exponential growth of the Hilbert space with the number of particles. As the system size increases, the number of possible quantum many-body states becomes so large that classical computers struggle to handle them efficiently [1, 2].

To overcome this challenge, quantum computation has started gaining popularity. It offers the potential to solve problems that classical computation cannot handle due to the possibility of simulating quantum states exploiting the basic properties of quantum mechanics, such as state superposition [1]. However, in the current Noisy Intermediate-Scale Quantum (NISQ) era, quantum computers are noisy and, to address this limitation, hybrid quantum-classical algorithms have been developed [3, 4]. These methods combine classical optimization techniques with quantum state superposition and measurement, which enables an efficient way to exploit the quantum resources available nowadays.

In this work, we apply a hybrid algorithm, the Adaptive Derivative-Assembled Pseudo-Trotter ansatz Variational Quantum Eigensolver (ADAPT-VQE) [4] to find the ground state of ^{6}Be, ^{12}C and ^{14}N nuclei. To do this task, I compute the ground state of these nuclei using the nuclear shell model in a simulation of a perfect quantum computer [5]. The aim of this work is the quantification of the unavoidable measurement error in ADAPT characteristic from quantum measurements. It also studies the interaction between this stochastic error with the classical optimization.

* amoronro30@alumnes.ub.edu
† menendez@fqa.ub.edu

II. NUCLEAR SHELL MODEL

The nuclear shell model describes nuclear structure by organizing nucleons into quantized energy shells. This model explains the empirical observation of magic numbers. These are the numbers of nucleons of particularly bound, stable nuclei. These magic numbers correspond to the complete filling of shells, which are separated by large energy gaps. According to the model, these filled shells form an inert inner core. Therefore, the study of nuclear structure focuses on the outermost shell (valence shell), which contains the active nucleons [2, 6].

With that in mind, we can create a single-particle basis within the valence shell. This space includes all orbitals the nucleons can occupy according to the Pauli exclusion principle [7]. This space is different for protons and neutrons, as the third component of the isospin is different for them. Each possible orbital is defined by particular quantum numbers: n, l_j and m. Coupling the nucleon's spin ($s = 1/2$) with its orbital angular momentum (l) generates the total angular momentum (j). In Fig. 1, we see the representation of the valence space in the p shell, which means $l = 1$ in spectroscopic notation. At the bottom, "m" refers to the third component of the total angular momentum of each single-particle state. Each j subshell has $2j + 1$ degenerate states. In total, the p shell in the valence space offers 6 possible single-particle orbitals for each type of nucleon.

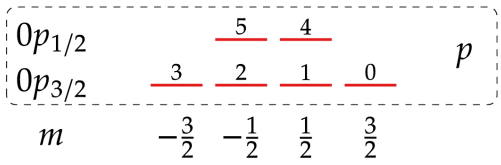

FIG. 1. Representation of the single-particle states in the p-shell valence space, labelled by nl_j and m (see the text for definitions) as well as their association with qubits (labelled above each level) under the Jordan-Wigner mapping (Eq. 5). Figure adapted from [5], under the CC BY 4.0 licence.

Using this single-particle basis, we can write the Hamiltonian of the nuclear system in a second quantization workframe,

$$\hat{H}_{eff} = \sum_{\alpha} \epsilon_\alpha \hat{a}^\dagger_\alpha \hat{a}_\alpha + \frac{1}{4} \sum_{\alpha\beta\gamma\delta} \overline{\nu}_{\alpha\beta\gamma\delta} \hat{a}^\dagger_\alpha \hat{a}^\dagger_\beta \hat{a}_\delta \hat{a}_\gamma, \quad (1)$$

where ϵ_α is the single-particle energy of the α state; $\overline{\nu}_{\alpha\beta\gamma\delta} = \nu_{\alpha\beta\gamma\delta} - \nu_{\alpha\beta\delta\gamma}$ are the antisimetrized two-body interaction coefficients; and $\hat{a}^\dagger_\alpha$ and $\hat{a}_\alpha$ are the creation and annihilation fermionic operators of state α [5]. For the p shell, we use the Cohen-Kurath interaction [8], which provides the single-particle energies and two-body matrix elements in units of MeV and accurately describes the nuclear structure of the ground states of these nuclei.

Solving the many-body problem demands finding the ground state of the system. While this is feasible with classical computers for p-shell nuclei, as the valence space grows, the number of different many-body basis states grows exponentially [2]. To address this challenge, ADAPT-VQE appears to be an interesting method with potential to be applicable to heavy nuclei [5]. As a preliminary step in this endeavour, in this work we analyse the performance of ADAPT in light nuclei.

III. ADAPT-VQE FOUNDATIONS

The ADAPT-VQE [4] was born to exploit NISQ devices capabilities. ADAPT-VQE uses quantum and classical computation resources. The method constructs the ground state ansatz by iteratively increasing its complexity from an initial reference state. This is achieved by sequentially applying unitary transformations, where each new operator and its corresponding variational parameter are selected according to the variational principle to ensure the minimization of the system's energy [4]:

$$|\Psi\rangle = \prod_{k=1}^{N} e^{i\theta_k \hat{A}_k} |ref\rangle \ , \quad (2)$$

where $|\Psi\rangle$ is the ansatz, θ_k are the different variational parameters, $\hat{A}_k$ are the operators, N is the number of ADAPT layers and $|ref\rangle$ is the reference state, which we take as a many-body Slater determinant, built from the single-particle basis in Fig. 1. It is important that these operators conserve all the symmetries of the system, mainly the third component of the total angular momentum and isospin of the nucleus, as the Hamiltonian is invariant to rotation [8]. The operators need to be antihermitian, so that the imaginary exponentials in Eq. 2 are unitary. With that in mind, we can define an "operator pool" with all the operators that fulfil this condition with the form of antihermitian two-particle-two-hole excitations,

$$\hat{T}^{rs}_{pq} = \hat{a}^\dagger_p \hat{a}^\dagger_q \hat{a}_r \hat{a}_s - \hat{a}^\dagger_r \hat{a}^\dagger_s \hat{a}_p \hat{a}_q. \quad (3)$$

The key point of the method is the selection of the A_k operators. Every time we add a new layer, we compute the energy gradient at $\theta_k = 0$ for every operator in the pool, and we select the one with the largest absolute value gradient. We compute the energy gradient,

$$\left.\frac{\partial E}{\partial \theta_k}\right|_{\theta_k=0} = i\langle\Psi_{k-1}| \left[\hat{H}_{eff}, \hat{T}^{rs}_{pq}\right] |\Psi_{k-1}\rangle, \quad (4)$$

where $|\Psi_{k-1}\rangle$ is the ansatz of the wave function after applying the $k-1$ operators. Then we optimize the parameters to minimize the energy. This optimization is done in a classical computer.

In consideration of that, we can explain the iterative execution flux:

1. Initialize ADAPT with a reference state ($|ref\rangle$) or with the state resulting from step 3.
2. Compute the energy gradient for all the operators in the operator pool (Eq. 4) and select the operator with the largest absolute value gradient. If the maximum gradient is lower than a previously set threshold, the energy has converged, so stop the algorithm.
3. Apply the unitary parametrized gate of the operator and classically optimize all the parameters classically. If it has reached a maximum amount of layers, stop the algorithm.

IV. ADAPT-VQE EXECUTION

Once we understand how ADAPT works, we need to resolve the following: the representation of the wave function on a quantum computer, the application of unitary operators, and the measurement of the nucleus's energy. The wave function of the system is represented by identifying the single-particle states in the valence shell with qubits. The occupation of a particular orbital translates to the state of the different qubits as $|0\rangle \equiv$ no occupation, $|1\rangle \equiv$ occupation. Using the notation of the orbitals used in Fig. 1 we need a quantum computer with as many qubits as orbitals in the valence shell. We need 6 qubits for p-shell simulations considering only one type of nucleon in the valence shell and 12 qubits if we consider neutrons and protons, regardless of the number of nucleons in the shell.

To apply the different operators to the reference state, we need to transform the operators to unitary quantum gates that we can use in our quantum circuit. This process starts by applying the Jordan-Wigner mapping [9] over the different $\hat{A}_k$. This transformation changes the creation and annihilation operators into a set of Pauli operators ($\hat{X}$, $\hat{Y}$ and $\hat{Z}$) applied over different qubits,

$$\hat{a}^\pm_i = \left(\prod_{p=0}^{i-1} \hat{Z}_p\right) \frac{1}{2} \left(\hat{X}_i \pm i\hat{Y}_i\right) \begin{cases} + \text{ for } \hat{a}_i \\ - \text{ for } \hat{a}^\dagger_i \end{cases} . \quad (5)$$

By doing this transformation, we obtain the different T^{rs}_{pq} as a sum of sets of Pauli strings, which I obtain using the python library "OpenFermion" [10]. All these Pauli strings commute with each other for all $\hat{T}^{rs}_{pq}$ type of operators [4], so we can represent $e^{i\theta\hat{T}^{rs}_{pq}}$ from Eq. 2 as the multiplication of individual imaginary Pauli-string exponentials.

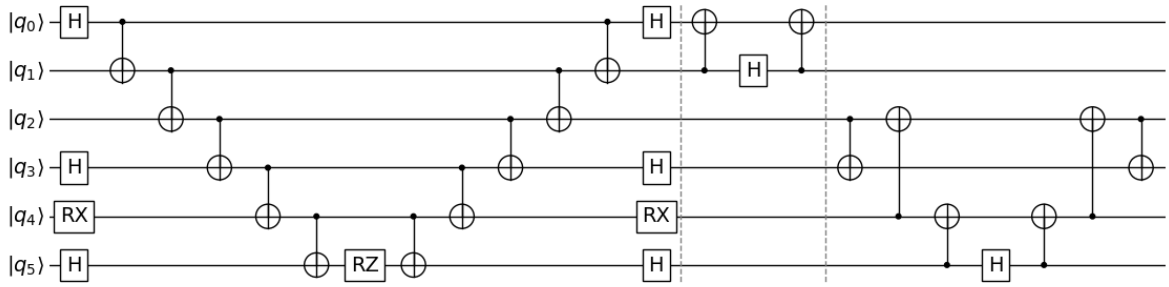

FIG. 2. Left: circuit representation of the imaginary exponential of the Pauli string $\hat{X}_0\hat{Z}_1\hat{Z}_2\hat{X}_3\hat{Y}_4\hat{X}_5$. This is one piece of the full unitary gate $e^{i\theta\hat{T}^{45}_{03}}$. Centre: the unitary gate M_{01}. Right: the unitary gate M_{2345}.

A. Ansatz quantum circuit and energy measurement

To obtain the quantum circuit to simulate the ansatz approximation of the ground state, we need to start by representing the reference state and then apply the unitary imaginary Pauli exponentials. To represent the reference state, we apply Pauli $\hat{X}$ gates to the qubits that have an occupied orbital in our reference state ($\hat{X}|0\rangle = |1\rangle$). For example, if we want to represent a state with one nucleon in the orbitals 1 and 2 (see Fig. 1) we need to apply:

$$|ref\rangle = \hat{X}_1\hat{X}_2|0\rangle^{\otimes\, N_{qbits}}. \tag{6}$$

Next, we apply the unitary transformations. We use the Jordan-Wigner transformation (Eq. 5) to express the fermionic operators as a set of imaginary Pauli exponentials. Now that we have the operators in this form, we can use the Staircase Protocol [11] to decompose each Pauli string exponential into a sequence of fundamental quantum gates. These gates include the CNOT (CX_{ij}), which inverts the target qubit (i) if the control qubit (j) is in the $|1\rangle$ state; the Hadamard (H) gate, which creates superpositions; the Rotation about the X-axis ($R_X(\theta)$); and the Rotation about the Z-axis ($R_Z(\theta)$) [12].

The Staircase Protocol proceeds by applying a H or $R_X(\pi/2)$ gate to qubits with a $\hat{X}$ or $\hat{Y}$ in the Pauli string exponential. This is followed by a CNOT gate "staircase" formation, a $R_Z(\theta)$ rotation on the last qubit, then the symmetrical inverse CNOTs structure and finally, H or $R_X^\dagger(\pi/2)$ gates on the same initial qubits [11]. The left part of Fig. 2 offers a visual representation.

After we have created the ansatz circuit, we need to perform the energy measurements. To do so, we can define the one- and two-body components of the Hamiltonian (without their respective amplitudes ϵ_α and $\overline{\nu}_{\alpha\beta\gamma\delta}$). As the Hamiltonian is Hermitian, we use its symmetries to define the observables [5]:

$$h_\alpha = \langle\Psi|\hat{a}^\dagger_\alpha\hat{a}_\alpha|\Psi\rangle, \tag{7}$$

$$h_{\alpha\beta\alpha\beta} = \langle\Psi|\hat{a}^\dagger_\alpha\hat{a}^\dagger_\beta\hat{a}_\alpha\hat{a}_\beta|\Psi\rangle, \tag{8}$$

$$h_{\alpha\beta\alpha\gamma} = \langle\Psi|\hat{a}^\dagger_\alpha\hat{a}^\dagger_\beta\hat{a}_\alpha\hat{a}_\gamma + \hat{a}^\dagger_\alpha\hat{a}^\dagger_\gamma\hat{a}_\alpha\hat{a}_\beta|\Psi\rangle, \tag{9}$$

$$h_{\alpha\beta\gamma\delta} = \langle\Psi|\hat{a}^\dagger_\alpha\hat{a}^\dagger_\beta\hat{a}_\gamma\hat{a}_\delta + \hat{a}^\dagger_\gamma\hat{a}^\dagger_\delta\hat{a}_\alpha\hat{a}_\beta|\Psi\rangle. \tag{10}$$

Using this notation, the energy of the system can be calculated as:

$$E = \sum_{\alpha=0}^{N_{qbits}-1} \epsilon_\alpha\, h_\alpha + \sum_{\alpha<\beta} \overline{\nu}_{\alpha\beta\alpha\beta}\, h_{\alpha\beta\alpha\beta} + \sum_{\alpha<\beta<\gamma} \overline{\nu}_{\alpha\beta\alpha\gamma}\, h_{\alpha\beta\alpha\gamma} + \sum_{\substack{\alpha<\beta,\ \gamma<\delta \\ (\alpha,\beta)<(\gamma,\delta)}} \overline{\nu}_{\alpha\beta\gamma\delta}\, h_{\alpha\beta\gamma\delta}. \tag{11}$$

The first two energy contributions are defined by the probability of single-orbital occupation (Eq. 7) and the negative of the joint probability for two-orbital occupation (Eq. 8). In our wave function analogy, it means the probability of qubit α or qubits $\alpha\beta$ of being in the $|1\rangle$ state simultaneously,

$$h_\alpha = p_1^{(\alpha)} \qquad , \qquad h_{\alpha\beta\alpha\beta} = -p_{11}^{(\alpha\beta)}. \tag{12}$$

These measurements are diagonal in the computational basis. This property allows their direct and simultaneous measurement from a single set of repeated executions of the ansatz state preparation circuit, without requiring any additional gates. Performing the measurement of the other terms (Eqs. 9 and 10) is more complicated, as they are not diagonal observables of the single-particle basis. To diagonalize the observables, we add a diagonalization appendix to the quantum circuit. These diagonalization appendices are the unitary gates $M_{\alpha\beta}$ and $M_{\alpha\beta\gamma\delta}$.

$$M_{\alpha\beta} \equiv \mathrm{CX}_{\beta\alpha} H_\beta \mathrm{CX}_{\beta\alpha}, \tag{13}$$

$$M_{\alpha\beta\gamma\delta} \equiv \mathrm{CX}_{\alpha\beta}\mathrm{CX}_{\gamma\alpha}\mathrm{CX}_{\delta\gamma} H_\delta \mathrm{CX}_{\delta\gamma}\mathrm{CX}_{\gamma\alpha}\mathrm{CX}_{\alpha\beta}. \tag{14}$$

The middle and right parts of Fig. 2 offer a visual representation of this diagonalizing gates. After adding this diagonalization part, we can measure the non-diagonal expected values as:

$$h_{\alpha\beta\alpha\gamma} = \sum_{n=0}^{2^{\text{num. }Z}} (-1)^n \left[p^{(Z,\alpha\beta\gamma)}_{\text{bin}(n),1\cdots10} - p^{(Z,\alpha\beta\gamma)}_{\text{bin}(n),1\cdots01}\right], \tag{15}$$

$$h_{\alpha\beta\gamma\delta} = \sum_{n=0}^{2^{\text{num. }Z}} (-1)^n \left[p^{(Z,\alpha\beta\gamma\delta)}_{\text{bin}(n),1\cdots1100} - p^{(Z,\alpha\beta\gamma\delta)}_{\text{bin}(n),1\cdots0011}\right], \tag{16}$$

where Z are all the qubits affected by the $\hat{Z}$ operators in Eq. 5, num. Z is the number of Z-affected qubits and bin(n) is the binary string of length num. Z associated to the index n of the summation [5].

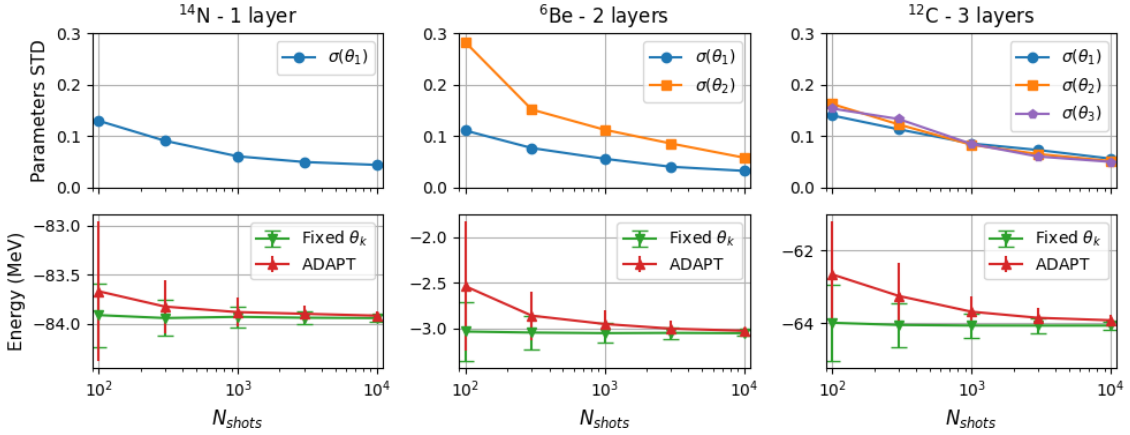

FIG. 3. Top panels: standard deviations of the parameters of the ADAPT ansatz from Eq. 2 as a function of the number of shots (N_{shots}). Bottom panels: energy of the ground state measured with fixed ideal parameters (green) and with a full ADAPT run (red) with their standard deviations error bars as a function of N_{shots}. The results correspond to calculations for ^{14}N (left panels), ^{6}Be (middle panels) and ^{12}C (right panels) nuclei.

Since the observable associated to $h_{\alpha\beta\alpha\gamma}$ commutes with similar observables with same β and γ indexes but different α, we can measure several of these contributions at the same time with the same circuit. This reduces by a large factor the number of necessary circuits to perform an energy measurement [5].

B. Error estimation and classical optimization

To measure, we make a series of observations (also called shots) of the final state and, with the result of each shot, we calculate the different probabilities in Eqs. 12, 15 and 16, so they are not infinitely precise measurements. This is an unavoidable error of the measurement process. As it is a probabilistic noise, it decreases proportional to the inverse of the square root of the number of shots, N_{shots} [5].

It is also worth discussing what type of classical optimization technique we should use to optimize the θ_k parameters. Although gradient based optimization methods are faster, they are not noise resistant [13]. For this reason, I have used the "COBYLA" optimizer from the SciPy python library [14].

V. RESULTS

I have studied how N_{shots} affects the accuracy of the energy measurements and the minimization. To perform the simulation of each quantum circuit, I have used the "Qibo" python framework [15]. I simulated a perfect quantum computer, which means I have not implemented any noisy channel, so the errors that appear are pure stochastic errors characteristic from statistical measurements. The different simulations have been done for the ^{6}Be, ^{12}C and ^{14}N nuclei. We need 13 circuits to do an energy measurement of ^{6}Be and 114 for ^{12}C and ^{14}N. These 3 nuclei have been selected because they are representative cases where a low relative energy error is achieved using one (^{14}N), two (^{6}Be), and three (^{12}C) ADAPT-VQE layers.

For each nucleus, I have run 200 ADAPT simulations for each N_{shots} to study how the values of the variational parameters and energy measurements vary from simulation to simulation. Fig. 3 presents the main results. The left panels show the simulation of ^{14}N with one ADAPT layer, the middle part, the simulation of ^{6}Be with two ADAPT layers and the right panels show the simulation of ^{12}C with three ADAPT layers. The top panels indicate the standard deviation of the different parameters as a function of the numbers of shots. The bottom panels show the energy measured by two different methods: in red, the mean energy measured for a full ADAPT simulation with its standard deviation error bar and, in green, the measured energy with fixed ideal parameters with its standard deviation error bar.

The lower panels in Fig. 3 highlight that the measured energy error with fixed parameters decreases with the number of shots, while the mean value is constant. The mean value agrees with the expected value for the measured energy with infinite precision. In accordance with the variational principle, this energy value is an upper bound to the ground state energy. Achieving greater precision for the ground state requires adding more ADAPT layers. On the other hand, the error decrease is proportional to $1/\sqrt{N_{shots}}$ for the three nuclei, consistent with the central limit theorem for statistical measurements.

However, when we implement a full ADAPT run, the trend is different. The error in this case is caused by two factors. The first one is the previously introduced statistical error. The other source of error is the noise in the optimization of the parameters. The interaction between the energy-measurement noise and classical optimization is hard to characterize. For these reasons, the energy error obtained with the full ADAPT run is larger than the one with fixed parameters, but it decreases faster with N_{shots}, following a power-law relationship that is determined by a log-log fit to the results. The error dependence for ^{14}N, ^{6}Be and ^{12}C is proportional to $(N_{shots})^{-0.53}$, $(N_{shots})^{-0.60}$ and $(N_{shots})^{-0.51}$, respectively.

Furthermore, the convergence behaviour in the

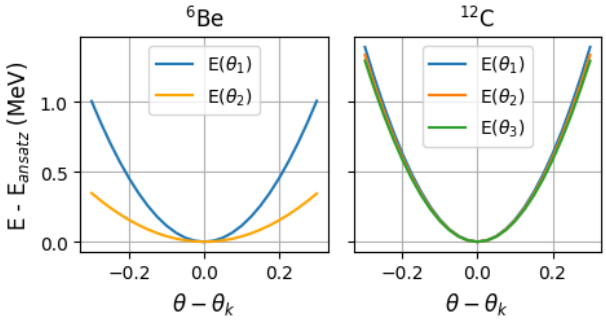

FIG. 4. Energy dependence of one parameter, with the other parameters fixed around the energy minimum. Left panel: result for ^{6}Be. Right panel: result for ^{12}C.

ADAPT-VQE energy is caused by the noise of the parameter optimization process. With noisy energy measurements, the optimization algorithm may prematurely stop, leading to suboptimal parameter values and, consequently, a higher mean measured energy. As N_{shots} increases, the noise in the parameters is reduced, allowing for a more accurate optimization, which translates into a mean energy closer to the ideal minimum.

Finally, the top panels of Fig. 3 show notable differences in parameter standard deviations. For the ^{6}Be nucleus, $\sigma(\theta_2)$ is significantly larger than $\sigma(\theta_1)$, contrasting with the ^{12}C results, where all three parameter deviations are similar. This discrepancy in parameter uncertainty is directly related to the curvature of the energy function around the minimum. A shallower curvature indicates that a wider range of parameter values correspond to a similar energy. Consequently, the statistical noise in the energy measurements can easily mislead the optimizer, leading to a greater uncertainty in the final parameter value. Conversely, a sharp curvature provides a well-defined minimum that is more robust against noise. As illustrated in Fig. 4, the energy dependence on each parameter around the minimum is different for the two parameters of ^{6}Be, whereas for the three parameters of ^{12}C, this dependency is very similar across them.

VI. CONCLUSIONS

In this work, I have successfully implemented the ADAPT-VQE (code available at my GitHub repository [16]) method to find the ground state of ^{6}Be, ^{12}C and ^{14}N nuclei within the nuclear shell model. The focus of this study is the investigation of statistical noise, inherent in quantum measurements, by varying the number of measurements (N_{shots}) one can perform in a quantum computer in order to obtain the energy of the ground state.

The results demonstrate that while the statistical error decreases as $(N_{shots})^{-0.5}$ for a single energy measurement, the statistical error of a full ADAPT simulation exhibits a more complex behaviour due to the interaction with the classical optimization process, resulting in a higher overall error that decreases with a distinct power dependence compared to the ideal statistical scaling. This power varies from nucleus to nucleus, in particular $(N_{shots})^{-0.53}$ for ^{14}N, $(N_{shots})^{-0.60}$ for ^{6}Be, and $(N_{shots})^{-0.51}$ for ^{12}C. Furthermore, the mean energy obtained from full ADAPT simulations converges towards the ideal minimum as N_{shots} increases. This indicates that the optimizer performs better with less noisy energy measurements.

Given that all the energy measurements have been performed over a simulation of a perfect quantum computer, the logical next step is executing ADAPT-VQE on actual quantum hardware. A systematic approach would start by performing energy measurements with fixed parameters to assess the direct impact of hardware noise on the experimental outcome. Afterwards, one should progressively incorporate ADAPT layers to study the interaction between the classical optimizer and the accumulating hardware noise, which naturally increases with the number of quantum gates. This would allow characterizing noise effects beyond those investigated in this work. These insights are valuable for guiding future efforts to implement variational quantum algorithms on real quantum hardware.

ACKNOWLEDGMENTS

I would like to sincerely thank Dr. Arnau Rios, Dr. Javier Menéndez, and Kerman Gallego for their support, guidance, and involvement throughout the course of this project. I also extend my gratitude to my family, particularly to my father and my partner, for their continued support and genuine interest during my working process.

[1] R. P. Feynman, Int. J. Theor. Phys. **21**, 467 (1982).
[2] E. Caurier *et al.*, Rev. Mod. Phys. **77**, 427 (2005).
[3] J. Preskill, Quantum **2**, 79 (2018).
[4] H. R. Grimsley *et al.*, Nat. Commun. **10**, 3007 (2019).
[5] A. Pérez-Obiol *et al.*, Sci. Rep **13**, 12291 (2023).
[6] M. G. Mayer and J. H. D. Jensen, *Elementary Theory of Nuclear Shell Structure* (Wiley, New York, 1955).
[7] W. Pauli, Z. Phys **31**, 765 (1925).
[8] S. Cohen and D. Kurath, Nucl. Phys. **73**, 1 (1965).
[9] P. Jordan and E. Wigner, Z. Phys. **47**, 631 (1928).
[10] J. R. McClean *et al.*, QST **5**, 034014 (2020).
[11] M. B. Mansky *et al.*, (2023), arXiv:2305.04807.
[12] A. Barenco *et al.*, Phys. Rev. A **52**, 3457 (1995).
[13] Pellow-Jarman *et al.*, Quantum Inf. Process **20**, 10.1007/s11128-021-03140-x (2021).
[14] P. Virtanen *et al.*, Nat. Methods **17**, 261 (2020).
[15] S. Efthymiou *et al.*, Quantum **6**, 814 (2022).
[16] A. Morón, `https://github.com/ArnauMoron/ADAPT-VQE` (2025).

Simulació de nuclis atòmics lleugers en un ordinador quàntic

Author: Arnau Morón Rodríguez
Facultat de Física, Universitat de Barcelona, Diagonal 645, 08028 Barcelona, Spain.[*]
Advisor: Javier Menéndez [†]

Resum: Resoldre la dinàmica de sistemes de molts cossos és un dels desafiaments més importants de la ciència moderna. Per aquesta aplicació, les tècniques de computació clàssica enfronten limitacions significatives, principalment la necessitat de gestionar grans espais de Hilbert. La computació quàntica, particularment a través d'algorismes híbrids quàntics i clàssics, ha començat a guanyar popularitat, oferint un enfocament nou i prometedor. Aquest treball caracteritza l'algorisme ADAPT-VQE ("Adaptive Derivative-Assembled Pseudo-Trotter ansatz Variational Quantum Eigensolver") mitjançant la simulació dels nuclis de ^{6}Be, ^{12}C i ^{14}N a través del model de capes en un ordinador quàntic ideal. Estudia específicament la resposta de l'ADAPT-VQE al soroll estadístic inherent que resulta del fet de fer un nombre finit de mesures ("shots"). En particular, l'estudi quantifica la convergència de l'error de mesura de l'energia amb el nombre de mesures, i demostra com el soroll estadístic afecta l'optimització dels paràmetres variacionals. Els resultats mostren que aquest impacte produeix un error final d'energia que escala amb N_{shots} segons una llei de potències diferent del límit estadístic estàndard i particular per a cada nucli. Paral·lelament, l'energia mitjana s'apropa al valor clàssicament calculat a mesura que el rendiment de l'optimitzador millora amb més nombre mesures.
Paraules clau: Computació quàntica, model de capes, VQE
ODSs: Educació de qualitat, Energia neta i sostenible i Industria, inovació, infraestructures

OBJECTIUS DE DESENVOLUPAMENT SOSTENIBLE (ODSS O SDGS)

TABLE I. Objectius de Desenvolupament Sostenible (ODSs o SDGs)

1. Fi de la es desigualtats		10. Reducció de les desigualtats	
2. Fam zero		11. Ciutats i comunitats sostenibles	
3. Salut i benestar		12. Consum i producció responsables	
4. Educació de qualitat	X	13. Acció climàtica	
5. Igualtat de gènere		14. Vida submarina	
6. Aigua neta i sanejament		15. Vida terrestre	
7. Energia neta i sostenible	X	16. Pau, justícia i institucions sòlides	
8. Treball digne i creixement econòmic		17. Aliança pels objectius	
9. Indústria, innovació, infraestructures	X		

El contingut d'aquest TFG s'associa amb l'ODS 4 (Educació de Qualitat), ja que fomenta el desenvolupament de competències tècniques avançades i promou la ciència oberta. Es relaciona també amb l'ODS 7 (Energia Neta i Sostenible), donat que els avenços en la simulació de nuclis atòmics poden contribuir a llarg termini a la millora de l'eficiència i la seguretat de l'energia nuclear. Addicionalment, es vincula amb l'ODS 9 (Indústria, Innovació i Infraestructures) per la seva contribució a la millora de la capacitat tecnològica i científica en el camp de la computació quàntica.

[*] amoronro30@alumnes.ub.edu
[†] menendez@fqa.ub.edu